

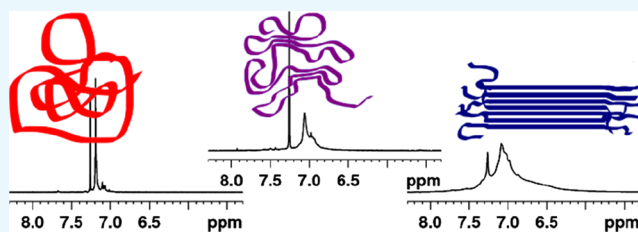
## π-Stacking Signature in NMR Solution Spectra of Thiophene-Based Conjugated Polymers

Francesca Parenti,<sup>†</sup> Francesco Tassinari,<sup>†,§</sup> Emanuela Libertini,<sup>†</sup> Massimiliano Lanzi,<sup>‡</sup> and Adele Mucci<sup>\*,†,§</sup>

<sup>†</sup>Dipartimento di Scienze Chimiche e Geologiche, Università di Modena e Reggio Emilia, Via G. Campi 103, 41125 Modena, Italy

<sup>‡</sup>Dipartimento di Chimica Industriale “Toso Montanari”, Università di Bologna, Viale del Risorgimento, 4, 40136 Bologna, Italy

**ABSTRACT:** Studies on conjugated polymers seldom report on their NMR characterization in solution. This paper shows how NMR experiments, both <sup>1</sup>H NMR and routine 2D NMR spectra, can help in gaining a further insight into the aggregation behavior of conjugated polymers and could be used to flank the more employed solid-state NMR and other spectroscopy and microscopy techniques in the understanding of the aggregation processes. NMR spectroscopy allows distinguishing, within the class of poorly solvatochromic conjugated polymers, those highly prone to form π-stacked aggregates from the ones that have a low tendency toward π-stacking.



### INTRODUCTION

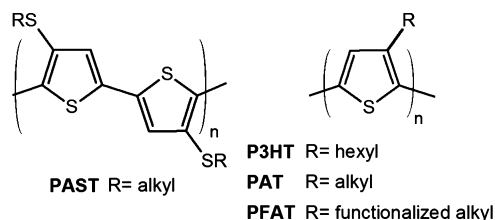
Thiophene-based conjugated polymers represent a widely studied class of polymers with broad applications in optoelectronics.<sup>1,2</sup> They are characterized by extended π-conjugated systems involving the whole polymer backbone and interacting with substituents, giving them the required optical and electronic properties. A variety of polythiophenes, differing in side-chain length and type, has been studied. β-Substituents make these polymers soluble and processable in organic solvents, in contrast to the unsubstituted polythiophene which is insoluble. One of the most employed conjugated polymers is poly(3-hexylthiophene), P3HT, which has been intensively studied during the last two decades and is still actively investigated.<sup>3</sup> The concept of conjugated polymers has extended during time to alternated copolymers, based on a variety of aromatic or heteroaromatic units with electron-donor or electron-acceptor characters.<sup>4</sup>

Both polythiophenes and thiophene-based polymers can be synthesized by a number of routes spanning from oxidative coupling with FeCl<sub>3</sub><sup>5</sup> to every kind of catalyzed cross-coupling reaction (e.g., Suzuki, Kumada, and Stille).<sup>6–8</sup> A number of books and papers on electro-optical properties and device characterization are found in the literature,<sup>1,2,9</sup> but only few of them report the solid-state NMR characterization of blends<sup>1,2,10–14</sup> or the in-depth NMR investigation of conjugated polymers in solution.<sup>15–23</sup> Indeed, papers dealing with the synthesis and characterization of conjugated polymers rarely report even their <sup>1</sup>H NMR spectra,<sup>14</sup> probably because of the discouraging broad line widths found, which seem to prevent a deep investigation.

We have been studying conjugated polymers for the last two decades, and from the beginning, we devoted our interest also to the in-depth 1D and 2D NMR characterization of alkyl-(PAT) and alkylsulfanyl-(PAST) polythiophenes (Chart

1)<sup>20,21,24–29</sup> that some of us reviewed in 2002.<sup>21</sup> These studies were mainly aimed at the assessment of the regiochemistry and

### Chart 1. Regioregular Polythiophenes



at the characterization of the minor configurational triads of polythiophenes. The polymer regiochemistry can, in fact, influence the conformation adopted by the backbone, which, in turn, is one of the factors ruling its aggregation behavior and electronic properties.<sup>30</sup>

As for the aggregation behavior in solution, it has been commonly investigated through ultraviolet–visible (UV–vis) spectroscopy. Some regioregular conjugated polymers, such as *head-to-tail* P3HT (and other PATs) and both *head-to-tail* and *head-to-head/tail-to-tail* PASTs, display marked solvatochromism and thermochromism.<sup>22,27,31–37</sup> They display an unstructured UV–vis absorption band in good solvents, which moves to a higher wavelength, assuming a vibrational fine structure upon the addition of a poor solvent (or upon cooling) or in the solid state (film). This behavior is attributed to the existence of an equilibrium process between a disordered, less extensively conjugated coil-like amorphous form, present in good solvents

Received: July 7, 2017

Accepted: August 30, 2017

Published: September 14, 2017

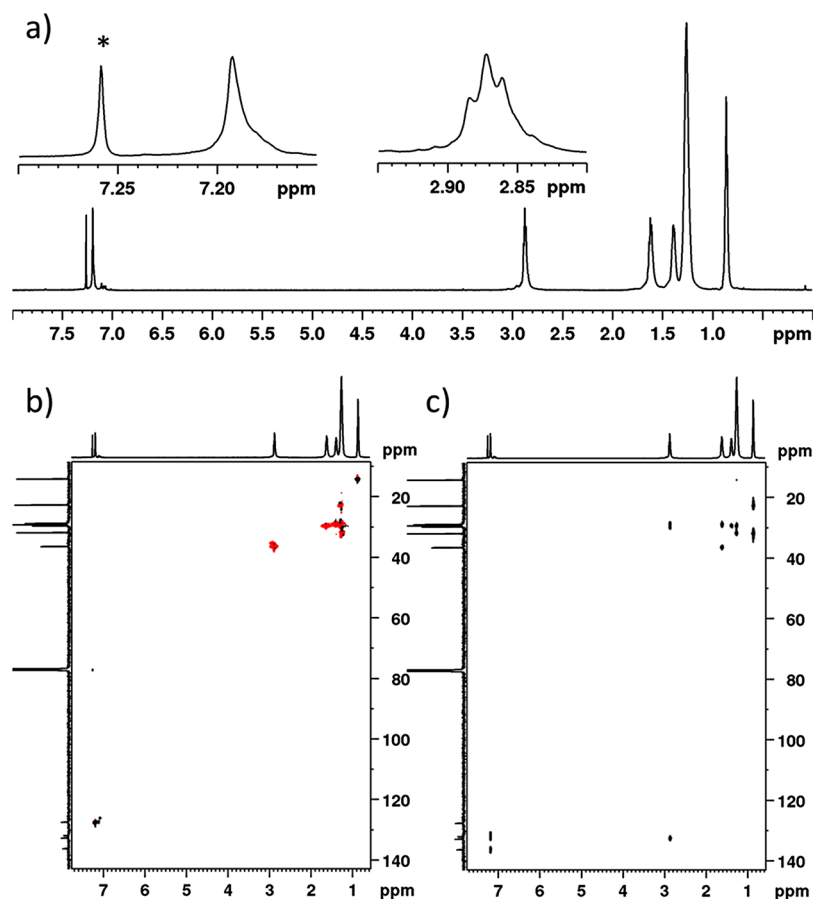


**Figure 1.** (a)  $^1\text{H}$  NMR spectrum in chloroform- $d$  (asterisk denotes the residual  $\text{CHCl}_3$  signal) and (b) HSQC and (c) HMBC spectra of a *head-to-head/tail-to-tail* regioregular PAST with  $R = \text{octyl chain}$  (PSOct).

or at high temperatures, and an ordered, more planar conjugated rodlike form prevailing in marginal solvents or at low temperatures. This last form is associated with the formation of small  $\pi$ -stacked aggregates. The nature of these aggregates still stimulates the interest of the scientific community<sup>32</sup> because the presence of  $\pi$ - $\pi$  interactions among PAT chains can induce some interesting behaviors, such as a secondary doping in conducting PATs,<sup>38</sup> a more extended conjugation length, which is responsible for a more extended UV-vis absorption spectrum as well as for a higher electrical conductivity,<sup>51</sup> and an increased charge carrier mobility,<sup>39</sup> particularly useful when the polymer is employed as an electron-donor material in polymeric solar cells. On the contrary, less regioregular polymers are also less solvatochromic.<sup>31,40–42</sup>

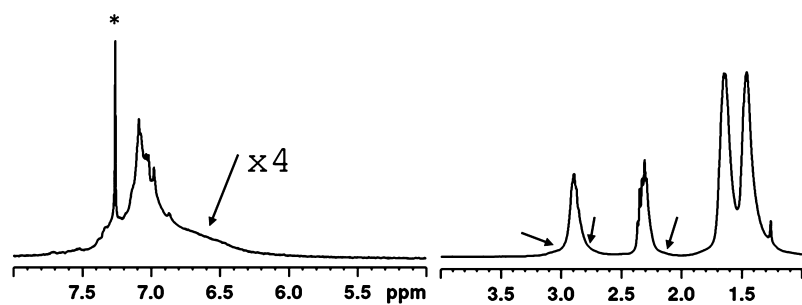
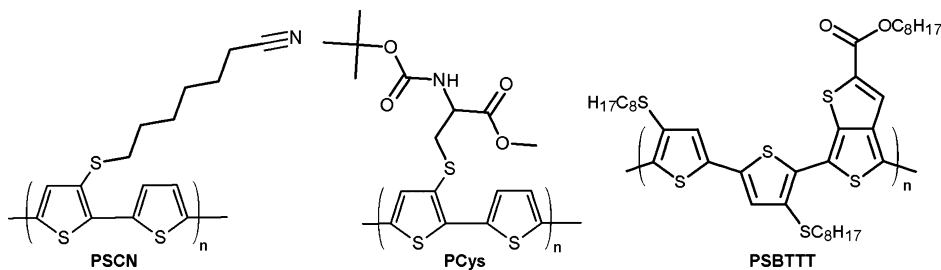
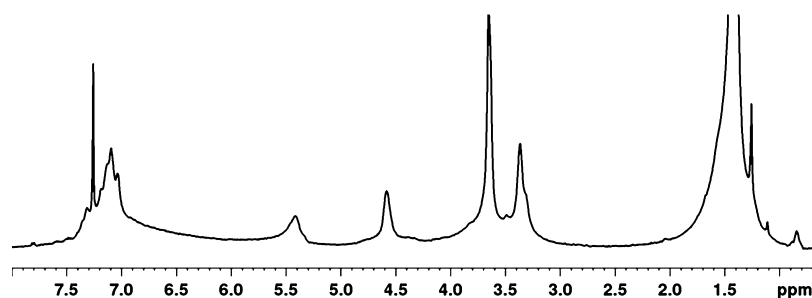
When we moved to the study of conjugated copolymers,<sup>15–20</sup> we observed that they were usually less solvatochromic than regioregular PATs and PASTs. This behavior can be explained either by a high tendency to planarize and aggregate even in good solvents or, on the contrary, by a low tendency toward aggregation, and this can strongly influence the properties of polymer-based devices.<sup>14,43</sup> We found that solution NMR can be very helpful in distinguishing between these two cases, and here we report on the NMR characterization of conjugated polymers in solution. NMR spectra obtained on polymer solutions can show characteristic signatures indicating if a poor solvatochromism is due to a high proneness to form  $\pi$ -stacked aggregates or not.

## RESULTS AND DISCUSSION

**NMR of Highly Solvatochromic Polymers.** We studied two classes of these polymers (Chart 1): highly regioregular P3HT<sup>28,29</sup> and regioregular PATs functionalized at the end of the side chains (PFATs) with hydroxy,<sup>44</sup> methoxy,<sup>45</sup> methylthio, hexylthio, methylsulfinyl, phenylsulfinyl,<sup>46</sup> piperidinyl, and hexanoyloxy groups<sup>47</sup> and PASTs.<sup>22,26,27</sup>

As mentioned above, regioregular *head-to-tail* PATs are found in a random coil conformation in chloroform solution by UV-vis spectroscopy. Their NMR spectra, obtained in the same (but deuterated) solvent, display slightly broader line widths (few hertz at half-height) with respect to those of small organic molecules, and the common 1D and 2D NMR experiments [correlation spectroscopy (COSY), total correlation spectroscopy (TOCSY), heteronuclear multiple-quantum coherence (HMQC), heteronuclear single-quantum coherence (HSQC), and heteronuclear multiple-bond correlation (HMBC)] can be exploited for their characterization. For instance, in the case of 85% *head-to-tail* regioregular P3HT, four sets of narrow aromatic proton<sup>48</sup> and carbon chemical shifts were assigned through HMQC and HMBC experiments to the four configurational triads and it was shown that their chemical shifts parallel those of the central units of the four isomeric trimers of 3-hexylthiophene.<sup>28,29</sup> We found a very similar situation for the solutions of regioregular PASTs, both for the *head-to-tail*<sup>26</sup> and for the *head-to-head/tail-to-tail* ones, one of which, carrying octylsulfanyl side chains (PSOct), is shown in Figure 1.<sup>22,27</sup>

Chart 2. Examples of Conjugated Polymers Displaying Aggregation Signatures in Their NMR Spectra

Figure 2.  $^1\text{H}$  NMR spectrum of PSCN, with broad signals marked by arrows, in chloroform- $d$  (asterisk denotes the residual  $\text{CHCl}_3$  signal).Figure 3.  $^1\text{H}$  NMR spectrum of PCys in chloroform- $d$ .

These polymers are more soluble in organic solvents than PATs, and their spectral lines are only slightly broader than those of small organic molecules. There are no problems in acquiring heterocorrelated spectra, both one bond and long range, and also in the obtainment of the directly acquired 1D  $^{13}\text{C}$  NMR spectra, provided a sufficient concentration is employed.

**NMR of Poorly Solvatochromic Polymers.** We came across two different classes of poorly solvatochromic polymers. The first class is formed by polythiophenes carrying alkylsulfanyl chains functionalized with polar groups every two thiophene rings and by copolymers containing thienothiophene and benzobithiophene units, such as those depicted in Chart 2.

The presence of an alkylsulfanyl chain carrying a polar group every other thienyl ring not only reduces the solvatochromism of these polythiophenes but also influences the appearance of their proton NMR spectra, which display both narrow and broad features,<sup>19,49</sup> as can be seen for the  $^1\text{H}$  NMR spectrum of PSCN, shown in Figure 2.

Very broad components, shielded with respect to the more narrow ones, appear in the aromatic region. These broad signals are due to the formation of aromatic  $\pi$ -stacks and derive from the mutual shielding effect of aromatic rings placed above or below to one another in these aggregates. Similar, even though less evident, spectral features are detected in the aliphatic

region for the portion of the alkyl chain bound to the heterocycle, indicating that it is affected by ring current shielding and deshielding phenomena.

More marked effects, leading to very broad spectral components, are observed when strongly interacting groups are present on the side chain, as in the case of a cysteine-substituted polythiophene (PCys),<sup>20,51</sup> the  $^1\text{H}$  NMR spectrum of which is shown in Figure 3, and of an ammonium-substituted polythiophene<sup>50</sup> (not shown). For these and other strongly aggregating polymers, the obtainment of  $^{13}\text{C}$  NMR aromatic signals is very time-consuming (whereas the aliphatic ones are usually detected), low proton–carbon correlations are detected in the aromatic region of HMQC or HSQC spectra (that probably derive from shorter chains or terminals), and HMBC spectra contain few long-range correlations for some of the aliphatic protons.

Nevertheless, a further insight into the structure of these aggregates can be obtained from proton homocorrelated spectra. Correlations through the space between the aromatic protons and the methylene protons bound to sulfur are found in the nuclear Overhauser effect spectroscopy (NOESY) spectrum (Figure 4) for both the narrow and the broad spectral components. These are intrasidue NOE detected in a more random coil or disordered form and in  $\pi$ -stack aggregates, respectively. The presence of these two forms is supported by gel permeation chromatography that shows a bimodal weight

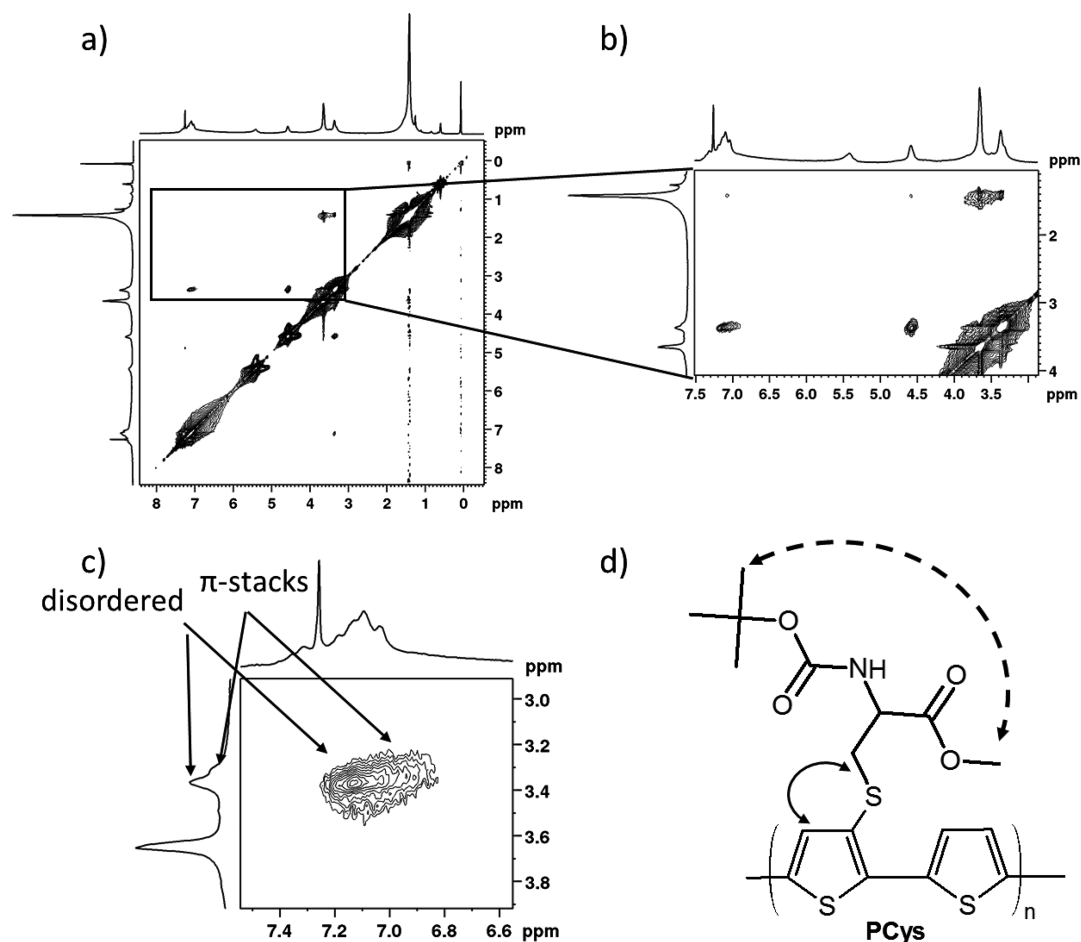


**Figure 4.** (a) NOESY spectrum of PCys in chloroform-*d*; (b) expanded region showing the dipolar interaction between SCH<sub>2</sub> and aromatic protons (further expanded in c) and that between *t*-butyl and methoxy signals (1.4 and 3.6 ppm, respectively); and (d) intrasidue (solid arrow) and interresidue (dashed arrow) dipolar correlations.

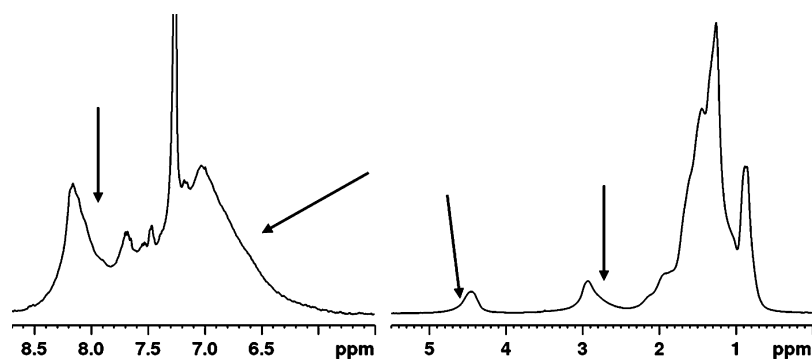


**Figure 5.** <sup>1</sup>H NMR spectrum of PSBTTT. The arrows evidence some broad spectral components in chloroform-*d*.

distribution.<sup>51</sup> Still in this NOESY spectrum, we find a strong NOE correlation between the methyl ester and the *t*-butyl carbamate groups that is due to an interresidue dipolar interaction due to the formation of hydrogen bonds.<sup>51</sup>

We observed a similar tendency to form  $\pi$ -stack aggregates in good solvents in other copolymers, containing thienothiophene and benzobithiophene units.<sup>15–17</sup> Also, these polymers display, together with a low solvatochromism when studied with UV–vis spectroscopy, broad components in their <sup>1</sup>H NMR spectra. Moreover, their aromatic carbon signals are difficult to detect, both in directly acquired 1D <sup>13</sup>C NMR spectra and through HSQC experiments, as in the case of PCys. Figure 5 shows the

<sup>1</sup>H NMR spectrum of a copolymer formed by alternating bithiophene and thienothiophene units<sup>16</sup> (PSBTTT in Chart 2), where broad and narrow components coexist.

A new and very intriguing feature of this last polymer is the effect of aggregation on the terminal part of the aliphatic chains. In fact, NMR revealed the presence of terminal CH<sub>2</sub>–CH<sub>2</sub>–CH<sub>3</sub> units shielded and deshielded with respect to the principal ones.<sup>16</sup> In particular, two groups of methyl signals appear in the HSQC spectrum of PSBTTT (Figure 6a) at about 0.9 (usual value) and 1.1 ppm (quite unusual). Their difference in proton chemical shifts is hardly justified by the different substitution at the opposite side of the long alkyl chains. Indeed, a closer

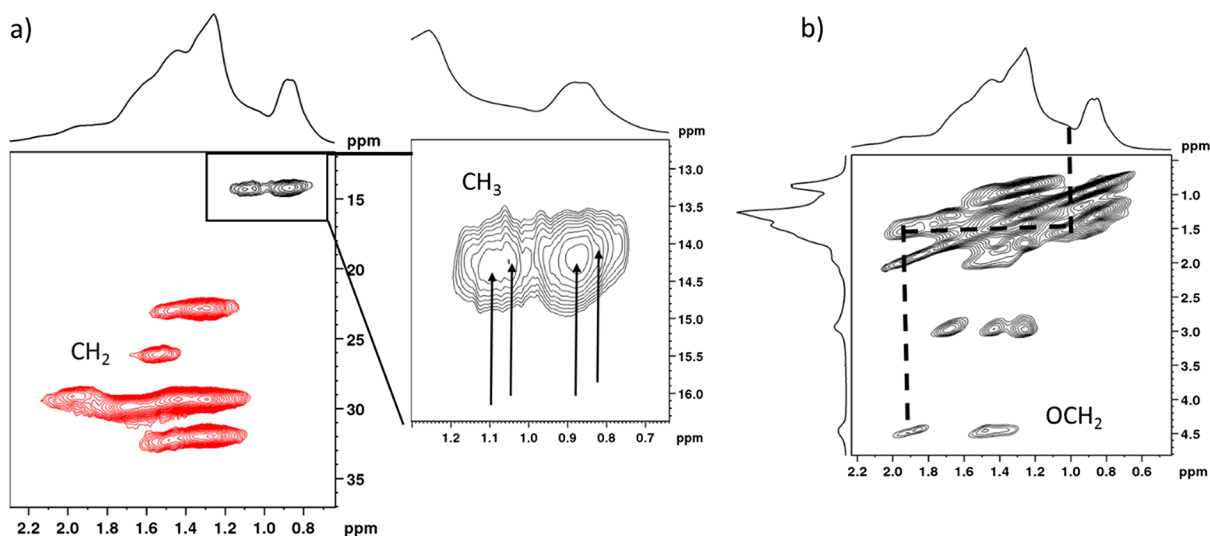


**Figure 6.** Partial (a) HSQC (the arrows point to multiple methyl signals) and (b) TOCSY (evidencing the correlation path that leads to the deshielded methyl signals) spectra of PSBTTT in chloroform-*d*.

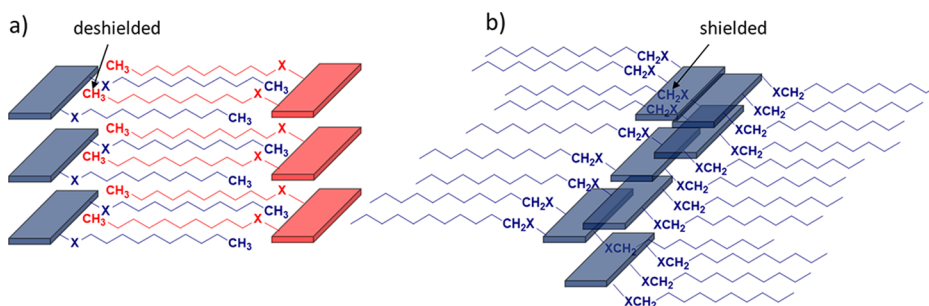


**Figure 7.** Sketches of (a) more ordered and (b) less ordered  $\pi$ -stacked arrangements in the polymer aggregates that can justify both shielding and deshielding of the initial and terminal protons of the substituents. In both cases, aromatic protons should be shielded.

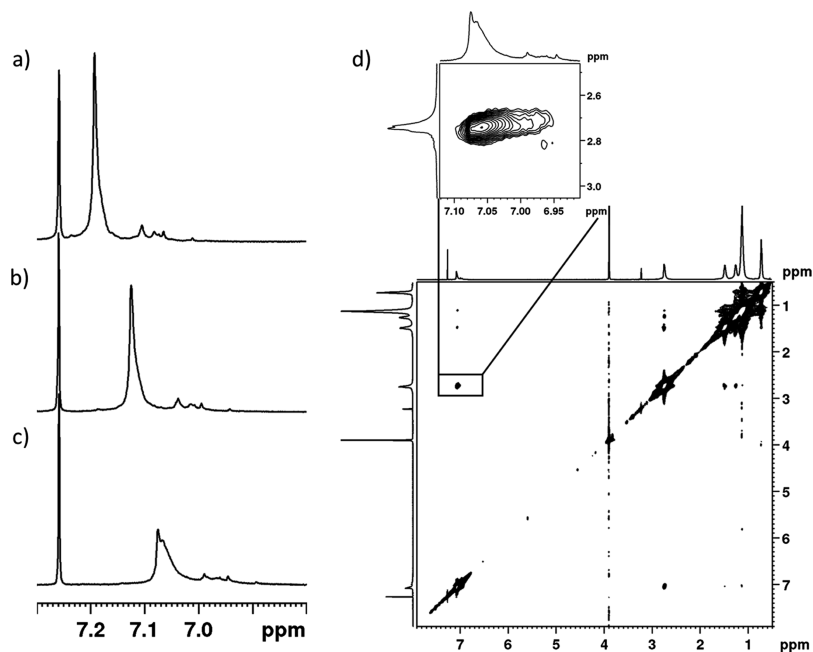


**Figure 8.** Changes in the  $^1\text{H}$  NMR spectra of PSOct upon the addition of methanol: (a) chloroform solution, (b) 20% (v/v) methanol, and (c) 30% (v/v) methanol. (d) NOESY spectrum at 30% (v/v) methanol.

inspection of the TOCSY spectrum shows that the deshielding involves some of the alkoxy chains (dashed path, Figure 6b)

and the methyl groups at 1.1 ppm belong to them. The minor signals coming from alkylsulfanyl chains are mainly found

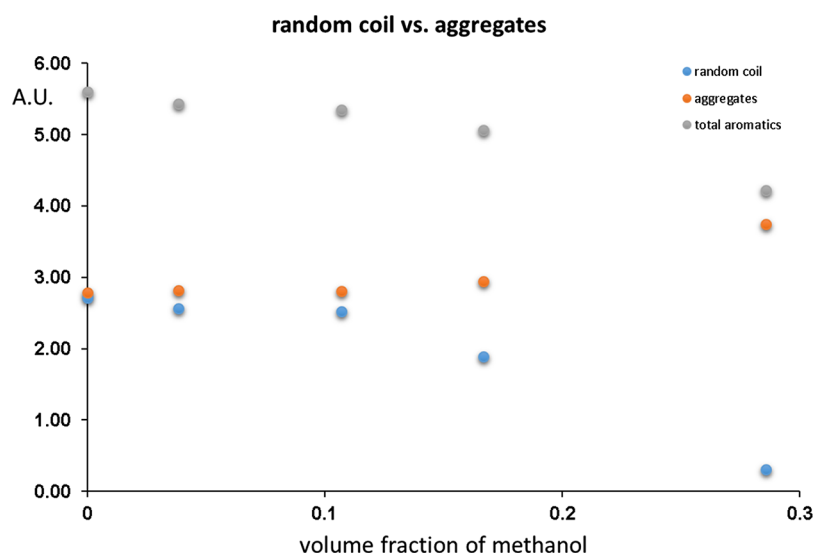


**Figure 9.** Changes of the integrals of narrow (orange, random coil), broad (blue,  $\pi$ -stacks), and total (gray) aromatic signals of PSOct due to the addition of deuterated methanol to a deuterated chloroform solution.

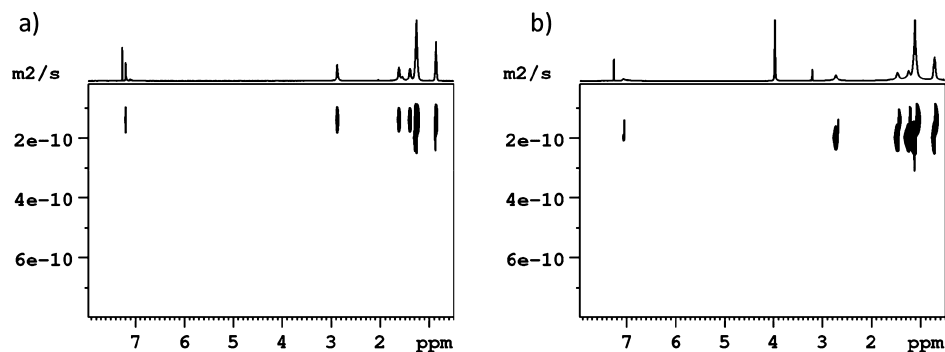


**Figure 10.** DOSY spectra of PSOct (a) in chloroform and (b) in 30% (v/v) methanol–chloroform mixture.

shielded with respect to the principal ones (right arrow in Figure 5).

To explain the presence of both shielded and deshielded signals for the alkyl groups close to the heteroatoms and deshielded signals for the alkyl terminals, we hypothesize that two types of aggregates are present (Figure 7). In the type shown in 7a, the alkyl chains are interdigitated between flanked highly ordered  $\pi$ -stacked aggregates, and both the initial and the terminal portions of the alkyl chains are forced to stay close to the deshielding zone of the aromatic rings of an adjacent stack. In the type shown in 7b, the polymer backbones are misaligned and the methylene groups bound to the heteroatoms are forced to stay either above or below the adjacent polymer backbone planes of the same less ordered  $\pi$ -stack and find themselves in a shielding region. In both cases, aromatic protons should be shielded.

The second class of poorly solvatochromic polymers is formed by regiorandom polythiophenes<sup>24,25,42,52–54</sup> and by copolymers containing the fluorene moiety.<sup>18,55</sup> The <sup>1</sup>H NMR spectra of these polymers are characterized by quite narrow line widths and the absence of shielded broad signals in the aromatic region. This behavior can be explained by a low proneness of these polymers to form  $\pi$ -stacked aggregates and by a tendency toward a random coil conformation even in aggregates.

**Aggregation Induced in Solvatochromic PSOct.** To understand if some aggregation process due to  $\pi$ -stacking could be evidenced for a solvatochromic polymer, regioregular PSOct<sup>27</sup> was investigated. When the <sup>1</sup>H NMR aromatic signal of PSOct is closely observed (Figure 8a), two components can be distinguished: one narrower and deshielded and the other broader and shielded, appearing as a shoulder. Also, four narrow and low shielded signals, which probably derive from terminal chlorinated bithienyl units, are found. This is not unexpected because it is known that chlorinated terminal units form when PATs are synthesized through oxidative coupling with FeCl<sub>3</sub>.<sup>56</sup>

Apart from a shift observed for all resonances (also for a trace of silicon and thus attributed to an unspecific interaction with the added solvent), a gradual broadening of the thienyl proton signals, a decrease of the intensity of the deshielded narrow component (Figure 8a,b), and an increase of the shielded shoulder are detected when methanol is added to a chloroform solution of PSOct. When the amount of methanol induces a persistent change in color of the solution (Figure 8c), the more shielded band becomes even broader. The integral of the global aromatic signals (with respect to that of residual CHCl<sub>3</sub>, used as an internal reference) also decreases, indicating the formation of some big aggregates characterized by transverse relaxation times  $T_2$ , too short to be detected by NMR. Integrals obtained by the deconvolution of the narrow deshielded aromatic proton

signal and of the broad components (Figure 9) are consistent with the gradual disappearance of the former and the enhancement of the latter, which were assigned by us to the resonances from random coil free chains and  $\pi$ -stacked aggregates, respectively. Signal deconvolution allows understanding that some aggregation (shielded shoulder) is already present in the chloroform solution at the concentration employed for NMR measurements (3 mg/mL, much higher than that used in UV-vis studies). A general broadening of the alkyl proton signals, more evident for those closer to sulfur, is also observed after the methanol addition.

An NOESY experiment allowed us to detect the dipolar (through space) interactions between aromatic and SCH<sub>2</sub> shielded and deshielded protons (Figure 8d). Note that the shape of the enlarged cross-peak in Figure 8d closely resembles that in Figure 4, although the extent of the broadening is lower for PSOct than those for PCys and for other strongly aggregating polymers,<sup>15–17,19</sup> such as those reported in Chart 2. As far as the terminal portion of the alkyl chains is concerned, no clear signs of trapping in aggregates were found for this polymer.

Eventually, diffusion-ordered spectroscopy (DOSY) experiments<sup>57</sup> were run on chloroform and on 30% (v/v) methanol–chloroform PSOct solutions (Figure 10), obtaining, quite unexpectedly, a higher self-diffusion coefficient in the latter case ( $1.7 \times 10^{-10}$  vs  $1.3 \times 10^{-10}$  m<sup>2</sup> s<sup>-1</sup> in chloroform). This is still more surprising if we consider that the viscosity of methanol–chloroform mixtures increases with respect to that of the pure solvents at high chloroform molar fractions.<sup>58</sup> Hypothesizing a similar behavior for the deuterated solvents, we interpolated a value of  $5.7 \times 10^{-4}$  kg m<sup>-1</sup> s<sup>-1</sup> for the viscosity of the employed solvent mixture (taking as a reference the viscosity of deuterated chloroform reported in ref 59). Employing the Stokes–Einstein equation for the translational diffusion coefficient,  $D = kT/(6\pi\eta r_H)$ , the diameters of the diffusing particles can be estimated to be around 6.4 and 4.5 nm in chloroform and in methanol–chloroform mixture, respectively. This means that the “aggregates” monitored by NMR for PSOct probably derive from an intrachain  $\pi$ -stacking process, similar to that described by Bartelt et al.,<sup>43</sup> rather than from a real interchain aggregation. An intrachain  $\pi$ -stacking process can explain the shrinking of the diameter of the diffusing particles observed by NMR.

## CONCLUSIONS

In this work, we focused on the NMR behavior of thiophene-based conjugated polymers and copolymers. We studied solution NMR spectra of three categories of conjugated polymers, mainly substituted with alkyl, functionalized alkyl, alkylsulfanyl, and functionalized alkylsulfanyl chains.

The first category is formed by highly solvatochromic and highly regioregular polythiophenes. They are present in good solvents as free chains, in a random coil conformation, and give 1D and 2D NMR spectra in chloroform as if they were small organic molecules, at least up to a number average molecular weight of 20 kDa, which was the highest we studied. These polymers planarize and aggregate in the presence of poor solvents and in films, as demonstrated by studies mainly based on UV-vis spectroscopy.

The second category is formed by polymers that display low solvatochromism and present, in the aromatic region of <sup>1</sup>H NMR spectra, broad shielded components that are due to the shielding induced by the  $\pi$ -stack formation on the aromatic

protons. The proneness to form  $\pi$ -stacked aggregates, even in good solvents, is at the base of the low solvatochromism of these polymers. Despite the large line widths, common 2D NMR experiments (HSQC, TOCSY, and NOESY) can still be used to gain a further insight into the structure of the aggregates.

Polymers that display low solvatochromism but do not present signs of aggregation in their NMR spectra form the third category. They are regiorandom polythiophenes and copolymers containing the fluorene units. For these polymers, the poor solvatochromism observed can be explained with a low tendency to form  $\pi$ -stacks in solution.

When aggregation is induced by the addition of a poor solvent to a solvatochromic polymer, PSOct, in chloroform solution, the signs of the formation of  $\pi$ -stacked structures can be detected. In fact, some spectral broadening of the aromatic resonances and the disappearance of the deshielded narrow component are observed. Furthermore, NMR shows that the terminal portions of the side chains seem not to be trapped in PSOct aggregates, at least the NMR-visible ones. Eventually, DOSY experiments indicate that the hydrodynamic radius of the NMR-visible aggregates is 30% lower than that of the random coil polymer chains. This finding suggests the formation of intrachain  $\pi$ -stacked regions rather than to a real interchain aggregation process, at least for the NMR-visible aggregates of PSOct.

In conclusion, in this paper, we showed that NMR spectra can be a valuable diagnostic tool for monitoring the proneness of conjugated polymers to form  $\pi$ -stacks. Details on these aggregates can be derived using 2D NMR experiments, which can be employed even when broad lines are present in <sup>1</sup>H NMR spectra. These experiments can be used in conjunction with other more employed techniques (UV-vis spectroscopy, small-angle X-ray scattering, solid-state NMR, atomic force microscopy, and scanning and transmission electron microscopy) to study the aggregation modes of conjugated polymers.

## EXPERIMENTAL SECTION

Table 1 summarizes the references to the synthesis and characterization of the polymers presented here and the data on their molecular weight distributions.

**Table 1. References, Weight Average Molecular Weight,  $M_w$ , Number Average Molecular Weight,  $M_n$ , and Polydispersity, PD, of the Polymers Reported Here**

polymer	references	$M_n$ (kDa)	$M_w$ (kDa)	PD
PSOct	27	20	70	3.5
PSCN	49	2.2, 17 <sup>a</sup>	2.7, 22 <sup>a</sup>	1.2, 1.3 <sup>a</sup>
PCys	20,51	93, 4.3 <sup>a</sup>	260, 6.0 <sup>a</sup>	2.8, 1.4
PSBTTT	16	8.0	17.0	2.4

<sup>a</sup>Minor component.

<sup>1</sup>H and <sup>13</sup>C NMR spectra were recorded with Bruker Avance 400 and Avance III HD 600 spectrometers, operated at 400.13 and 600.13 for proton and at 100.61 and 150.90 MHz for carbon, respectively, using standard pulse sequences on 3–10 mg/mL solutions. Two-dimensional TOCSY spectra (mlevetgp) were acquired using 1 s relaxation delay, 60–100 ms mixing (spin-lock) time, 10–20 ppm spectral width, 2–4k data points, 8–32 scans per increment, and 256 increments. Two-dimensional NOESY spectra (noesygpph) were acquired using 1 s relaxation delay, 50–100 ms mixing time, 10–20 ppm

spectral width, 2–4k data points, 24 scans per increment, and 256 increments. Two-dimensional echo–antiecho phase-sensitive HSQC edited spectra (hsqcedetgppsp) were acquired using 0.5 s relaxation delay, 1.6 ms evolution time, 10 ppm spectral width in f2, 2k data points, 16–96 scans per increment, 160 ppm spectral width in f1, and 160–400 increments. Two-dimensional HMBC spectra (hmbcgpplndqf) were acquired using 0.5 s relaxation delay, a 2.9 ms low-pass J filter, 50–100 ms evolution time, 10 ppm spectral width in f2, 4k data points, 32–160 scans per increment, 160–180 ppm spectral width in f1, and 160–400 increments. DOSY experiments were performed at 298 K, on 5 mm NMR tubes spinning at 20 Hz, using a stimulated echo sequence incorporating bipolar gradient pulses and a longitudinal eddy current delay (ledbpgp2s), 250 ms diffusion time (big delta), 5 ms longitudinal eddy current delay ( $T_e$ ),  $2 \times 1 - 1.5$  ms  $\delta$  (little delta), and 64 linear gradient ramp, with a maximum strength of  $58 \text{ G cm}^{-1}$ , followed by a gradient pulse recovery time of 200  $\mu\text{s}$ . After Fourier transformation and baseline correction, the diffusion dimension of the 2D DOSY spectra was processed by means of the Bruker TopSpin 3.5 software package. Deconvolution of  $^1\text{H}$  NMR spectra was done with Mnova 9.1.0 software (2012 Mestrelab Research S.L., Santiago de Compostela, Spain).

## AUTHOR INFORMATION

### Corresponding Author

\*E-mail: [adele.mucci@unimore.it](mailto:adele.mucci@unimore.it) (A.M.).

### ORCID

Adele Mucci: [0000-0003-3303-8761](https://orcid.org/0000-0003-3303-8761)

### Present Address

<sup>§</sup>Department of Chemical Physics, Weizmann Institute of Science, Rehovot 76100, Israel (F.T.).

### Author Contributions

The manuscript was written through the contributions of all authors. All authors have given approval to the final version of the manuscript.

### Notes

The authors declare no competing financial interest.

## ACKNOWLEDGMENTS

Fondazione Cassa di Risparmio di Modena is greatly acknowledged for funding the acquisition of the Bruker 600 MHz NMR spectrometer. The authors acknowledge the Università di Modena e Reggio Emilia for funds to A.M. [Linee Caratterizzanti di Ateneo UNIMORE 2011–2013 Nano- and emerging materials and systems for sustainable technologies].

## REFERENCES

- (1) *Handbook of Thiophene-Based Materials: Applications in Organic Electronics and Photonics*; Perepichka, I. F., Perepichka, D. F., Eds.; John Wiley & Sons, Ltd.: Chichester, 2009.
- (2) *Conjugated Polymers: Processing and Applications*; Skotheim, T. A., Reynolds, J., Eds.; CRC Press: Boca Raton, 2007.
- (3) *P3HT Revisited—From Molecular Scale to Solar Cell Devices*; Ludwigs, S., Ed.; Advances in Polymer Science, 265; Springer-Verlag, Berlin, Heidelberg: Germany, 2014.
- (4) Nakabayashi, K.; Mori, H. Donor–Acceptor Block Copolymers: Synthesis and Solar Cell Applications. *Materials* **2014**, *7*, 3274–3290.
- (5) Niemi, V. M.; Knuutila, P.; Österholm, J.-E.; Korvola, J. Polymerization of 3-alkylthiophenes with  $\text{FeCl}_3$ . *Polymer* **1992**, *33*, 1559–1562.
- (6) Li, C.; Bo, Z. New Chemistry for Organic Photovoltaic Materials. In *Polymer Photovoltaics: Materials, Physics, and Device Engineering*; Huang, F., Yip, H.-L., Cao, Y., Eds.; Royal Society of Chemistry: London, UK, 2015; pp 1–31.
- (7) Osaka, I.; McCullough, R. D. Advances in Molecular Design and Synthesis of Regioregular Polythiophenes. *Acc. Chem. Res.* **2008**, *41*, 1202–1214.
- (8) Anand, V.; Ramachandran, E.; Dhamodharan, R. Conjugated Polymers with Carbazole, Fluorene, and Ethylene Dioxithiophene in the Main Chain and a Pendant Cyano Group: Synthesis, Photo-physical, and Electrochemical Studies. *J. Polym. Sci., Part A: Polym. Chem.* **2016**, *54*, 2774–2784.
- (9) *Handbook of Organic Materials for Optical and (Opto)electronic Devices*; Ostroverkhova, O., Ed.; Woodhead Publishing, Ltd.: Cambridge, 2013.
- (10) Graham, K. R.; Cabanetos, C.; Jahnke, J. P.; Idso, M. N.; El Labban, A.; Ndjawa, G. O. N.; Heumueller, T.; Vandewal, K.; Salleo, A.; Chmelka, B. F.; Amassian, A.; Beaujuge, P. M.; McGehee, M. D. Importance of the Donor:Fullerene Intermolecular Arrangement for High-Efficiency Organic Photovoltaics. *J. Am. Chem. Soc.* **2014**, *136*, 9608–9618.
- (11) Beaujuge, P. M.; Tsao, H. N.; Hansen, M. R.; Amb, C. M.; Risko, C.; Subbiah, J.; Choudhury, K. R.; Mavrinskiy, A.; Pisula, W.; Brédas, J.-L.; So, F.; Müllen, K.; Reynolds, J. R. Synthetic Principles Directing Charge Transport in Low-Band-Gap Dithienosilole–Benzothiadiazole Copolymers. *J. Am. Chem. Soc.* **2012**, *134*, 8944–8957.
- (12) Dudenko, D.; Kiersnowski, A.; Shu, J.; Pisula, W.; Sebastiani, D.; Spiess, H. W.; Hansen, M. R. A Strategy for Revealing the Packing in Semicrystalline  $\pi$ -Conjugated Polymers: Crystal Structure of Bulk Poly-3-hexyl-thiophene (P3HT). *Angew. Chem., Int. Ed.* **2012**, *51*, 11068–11072.
- (13) Yuan, Y.; Shu, J.; Kolman, K.; Kiersnowski, A.; Bubeck, C.; Zhang, J.; Hansen, M. R. Multiple Chain Packing and Phase Composition in Regioregular Poly(3-butylthiophene) Films. *Macromolecules* **2016**, *49*, 9493–9506.
- (14) Warnan, J.; Cabanetos, C.; El Labban, A.; Hansen, M. R.; Tassone, C.; Toney, M. F.; Beaujuge, P. M. Ordering Effects in Benzo[1,2-b:4,5-b']difuran-thieno[3,4-c]pyrrole-4,6-dione Polymers with >7% Solar Cell Efficiency. *Adv. Mater.* **2014**, *26*, 4357–4362.
- (15) Parenti, F.; Ricciardi, R.; Diana, R.; Morvillo, P.; Fontanesi, C.; Tassinari, F.; Schenetti, L.; Minarini, C.; Mucci, A. Polymers for Application in Organic Solar Cells: Bithiophene Can Work Better than Thienothiophene when Coupled to Benzodithiophene. *J. Polym. Sci., Part A: Polym. Chem.* **2016**, *54*, 1603–1614.
- (16) Morvillo, P.; Diana, R.; Fontanesi, C.; Ricciardi, R.; Lanzi, M.; Mucci, A.; Tassinari, F.; Schenetti, L.; Minarini, C.; Parenti, F. Low band gap polymers for application in solar cells: synthesis and characterization of thienothiophene–thiophene copolymers. *Polym. Chem.* **2014**, *5*, 2391–2400.
- (17) Morvillo, P.; Parenti, F.; Diana, R.; Fontanesi, C.; Mucci, A.; Tassinari, F.; Schenetti, L. A novel copolymer from benzodithiophene and alkylsulfanyl-bithiophene: synthesis, characterization and application in polymer solar cells. *Sol. Energy Mater. Sol. Cells* **2012**, *104*, 45–52.
- (18) Parenti, F.; Morvillo, P.; Bobeico, E.; Diana, R.; Lanzi, M.; Fontanesi, C.; Tassinari, F.; Schenetti, L.; Mucci, A. (Alkylsulfanyl)-bithiophene-alt-Fluorene:  $\pi$ -Conjugated Polymers for Organic Solar Cells. *Eur. J. Org. Chem.* **2011**, 5659–5667.
- (19) Cagnoli, R.; Lanzi, M.; Libertini, E.; Mucci, A.; Paganin, L.; Parenti, F.; Preti, L.; Schenetti, L. Organic- and Water-Soluble Aminoalkylsulfanyl Polythiophenes. *Macromolecules* **2008**, *41*, 3785–3792.
- (20) Cagnoli, R.; Lanzi, M.; Mucci, A.; Parenti, F.; Schenetti, L. Polymerization of Cysteine Functionalized Thiophenes. *Polymer* **2005**, *46*, 3588–3596.
- (21) Schenetti, L.; Mucci, A. Inverse detection applied to the  $^1\text{H}$  and  $^{13}\text{C}$  assignment and to the regiochemical characterization of  $\beta$ -substituted  $\alpha, \alpha'$  coupled oligo- and polythiophenes. In *New Advances*



in *Analytical Chemistry*; Atta-ur-Rahman, Ed.; Taylor&Francis: London, 2002; Vol. 3, pp 1–40, and references herein.

(22) Iarossi, D.; Mucci, A.; Parenti, F.; Schenetti, L.; Seeber, R.; Zanardi, C.; Forni, A.; Tonelli, M. Synthesis and Spectroscopic and Electrochemical Characterisation of a Conducting Polythiophene bearing a Chiral  $\beta$ -Substituent. Polymerisation of (+)-4,4'-Bis[(S)-2-methylbutylsulfanyl]-2,2'-bithiophene. *Chem. Eur. J.* **2001**, *7*, 676–685.

(23) Van Mierloo, S.; Chambon, S.; Boyukbayram, A. E.; Adriaensens, P.; Lutsen, L.; Cleij, T. J.; Vanderzande, D. Synthesis,  $^1\text{H}$  and  $^{13}\text{C}$  NMR assignment and electrochemical properties of novel thiophene–thiazolothiazole oligomers and polymers. *Magn. Reson. Chem.* **2010**, *48*, 362–369.

(24) Goldoni, F.; Iarossi, D.; Mucci, A.; Schenetti, L.; Costa Bizzarri, P.; Della Casa, C.; Lanzi, M. Regiochemistry Characterization of Poly(3-hexanoyloxyethyl-2,5-thienylene) through Proton and Carbon Nuclear Magnetic Resonance Spectroscopy. *Polymer* **1997**, *38*, 1297–1302.

(25) Iarossi, D.; Mucci, A.; Schenetti, L.; Costa Bizzarri, P.; Della Casa, C.; Lanzi, M.  $^1\text{H}$  and  $^{13}\text{C}$  NMR characterization of poly[3-(6-methoxyhexyl)-2,2'-bithiophene]. *Magn. Reson. Chem.* **1999**, *37*, 182–188.

(26) Goldoni, F.; Iarossi, D.; Mucci, A.; Schenetti, L.; Zambianchi, M. Synthesis and Characterization of Poly[3-(Butylthio)Thiophene]: a Regioregular Head-to-Tail Polymer. *J. Mater. Chem.* **1997**, *7*, 593–596.

(27) Iarossi, D.; Mucci, A.; Schenetti, L.; Seeber, R.; Goldoni, F.; Affronte, M.; Nava, F. Polymerization and Characterization of 4,4'-bis(alkylsulfanyl)-2,2'-bithiophenes. *Macromolecules* **1999**, *32*, 1390–1397.

(28) Ferrari, M.; Mucci, A.; Schenetti, L.; Malmusi, L. Complete Assignment of the Aliphatic Chains in Dimers, Trimers and Polymer of 3-Hexylthiophene through 2D-NMR Spectroscopy. *Magn. Reson. Chem.* **1995**, *33*, 657–663.

(29) Mucci, A.; Schenetti, L.  $^1\text{H}$ - $^{13}\text{C}$  NMR inverse detection of poly(3-hexylthiophene): characterization of the structural defects. *Macromol. Chem. Phys.* **1995**, *196*, 2687–2693.

(30) Chen, T.-A.; Wu, X.; Rieke, R. D. Regiocontrolled Synthesis of Poly(3-alkylthiophenes) Mediated by Rieke Zinc: Their Characterization and Solid-state Properties. *J. Am. Chem. Soc.* **1995**, *117*, 233–244.

(31) Sandstedt, C. A.; Rieke, R. D.; Eckhardt, C. J. Solid-state and Solvatochromic Spectra of a Highly Regular Polythiophene. *Chem. Mater.* **1995**, *7*, 1057–1059.

(32) Panzer, F.; Sommer, M.; Bässler, H.; Thelakkat, M.; Köhler, A. Spectroscopic Signature of Two Distinct H-Aggregate Species in Poly(3-hexylthiophene). *Macromolecules* **2015**, *48*, 1543–1553.

(33) Johnson, C. E.; Boucher, D. S. Poly(3-hexylthiophene) Aggregate Formation in Binary Solvent Mixtures: An Excitonic Coupling Analysis. *J. Polym. Sci., Part B: Polym. Phys.* **2014**, *52*, 526–538.

(34) Yang, C.; Orfino, F. P.; Holdcroft, S. A Phenomenological Model for Predicting Thermochromism of Regioregular and Non-regioregular Poly(3-alkylthiophenes). *Macromolecules* **1996**, *29*, 6510–6517.

(35) Bertinelli, F.; Costa-Bizzarri, P.; Della-Casa, C.; Lanzi, M. Analysis of UV–Vis spectral profiles of solvatochromic poly[3-(10-hydroxydecyl)-2,5-thienylene]. *Spectrochim. Acta, Part A* **2002**, *58*, 583–592.

(36) Lanzi, M.; Della-Casa, C.; Costa-Bizzarri, P.; Bertinelli, F. Anomalous solvatochromic effect. Comparison between decyl and  $\omega$ -hydroxydecyl 3-substituted polythiophenes. *Macromol. Chem. Phys.* **2001**, *202*, 1917–1923.

(37) Bertinelli, F.; Costa-Bizzarri, P.; Della-Casa, C.; Lanzi, M. Solvent and temperature effects on the chromic behaviour of poly[3-(10-hydroxydecyl)-2,5-thienylene]. *Synth. Met.* **2001**, *122*, 267–273.

(38) Wu, C.-G.; Chien, L.-N. The  $\pi$ – $\pi$  interaction induced secondary doping in conducting poly-3-alkylthiophenes. *Synth. Met.* **2000**, *110*, 251–255.

(39) Park, Y. D.; Lee, H. S.; Choi, Y. J.; Kwak, D.; Cho, J. H.; Lee, S.; Cho, K. Solubility-Induced Ordered Polythiophene Precursors for

High-Performance Organic Thin-Film Transistors. *Adv. Funct. Mater.* **2009**, *19*, 1200–1206.

(40) Lanzi, M.; Costa Bizzarri, P.; Della Casa, C. Solvatochromic Properties of Poly[3-(6-methoxyhexyl)-2,5-thienylene] in different solvent mixtures. *Synth. Met.* **1997**, *89*, 181–186.

(41) Paganin, L.; Costa-Bizzarri, P.; Lanzi, M.; Cesari, G.; Bertinelli, F.; Cagnoli, R.; Mucci, A. Novel thiophenic copolymer as a multi-purpose macromolecular intermediate. *Macromol. Symp.* **2006**, *234*, 76–86.

(42) Costa-Bizzarri, P.; Della-Casa, C.; Lanzi, M.; Bertinelli, F.; Iarossi, D.; Mucci, A.; Schenetti, L. Spectroscopic comparison between poly[3-(6-methoxyhexyl)thiophene]s with different steric hindrance. *Synth. Met.* **1999**, *104*, 1–7.

(43) Bartelt, J. A.; Douglas, J. D.; Mateker, W. R.; El Labban, A.; Tassone, C. J.; Toney, M. F.; Fréchet, J. M. J.; Beaujuge, P. M.; McGehee, M. D. Controlling Solution-Phase Polymer Aggregation with Molecular Weight and Solvent Additives to Optimize Polymer-Fullerene Bulk Heterojunction Solar Cells. *Adv. Energy Mater.* **2014**, *4*, 1301733.

(44) Lanzi, M.; Costa-Bizzarri, P.; Della-Casa, C.; Paganin, L.; Fraleoni, A. Synthesis, characterization and optical properties of a regioregular and soluble poly[3-(10-hydroxydecyl)-2,5-thienylene]. *Polymer* **2003**, *44*, 535–545.

(45) Lanzi, M.; Paganin, L. Study of the order-disorder transitions in methoxy-functionalized polyalkylthiophenes. *Eur. Polym. J.* **2008**, *44*, 3987–3996.

(46) Lanzi, M.; Paganin, L. New regioregular polythiophenes functionalized with sulfur-containing substituents for bulk heterojunction solar cells. *React. Funct. Polym.* **2010**, *70*, 346–360.

(47) Lanzi, M.; Costa-Bizzarri, P.; Paganin, L.; Cesari, G. Synthesis by post-polymerization functionalization of sensitive polythiophenes for selective chemo-recognition purposes. *React. Funct. Polym.* **2007**, *67*, 329–340.

(48) Barbarella, G.; Bongini, A.; Zambianchi, M. Regiochemistry and Conformation of Poly(3-hexylthiophene) via the Synthesis and the Spectroscopic Characterization of the Model Configurational Triads. *Macromolecules* **1994**, *27*, 3039–3045.

(49) Cagnoli, R.; Mucci, A.; Parenti, F.; Schenetti, L.; Borsari, M.; Lodi, A.; Ponterini, G. A poly(alkylsulfanyl)thiophene functionalized with carboxylic groups. *Polymer* **2006**, *47*, 775–784.

(50) Cagnoli, R.; Caselli, M.; Libertini, E.; Mucci, A.; Parenti, F.; Ponterini, G.; Schenetti, L. Aggregation behaviour of a water-soluble ammonium-functionalized polythiophene: Luminescence enhancement induced by bile-acid anions. *Polymer* **2012**, *53*, 403–410.

(51) Mucci, A.; Parenti, F.; Schenetti, L. A Self-Assembling Polythiophene Functionalised with a Cysteine Moiety. *Macromol. Rapid Commun.* **2003**, *24*, 547–550.

(52) Lanzi, M.; Costa Bizzarri, P.; Paganin, L.; Cesari, G. Highly Processable ester-functionalized polythiophenes as valuable multifunctional and post-functionalizable conjugated polymers. *Eur. Polym. J.* **2007**, *43*, 72–83.

(53) Lanzi, M.; Bertinelli, F.; Costa-Bizzarri, P.; Paganin, L.; Cesari, G. Tuning of the electronic properties of self-assembling and highly sensitive chromic polyalkylthiophenes. *Eur. Polym. J.* **2007**, *43*, 835–846.

(54) Lanzi, M.; Costa Bizzarri, P.; Paganin, L.; Cesari, G. A new polythiophene derivative with highly sensitive and selective affinitychromism properties. *Synth. Met.* **2007**, *157*, 719–725.

(55) Kmínek, I.; Výprachtický, D.; Kříž, J.; Dybal, J.; Cimrová, V. Low-Band Gap Copolymers Containing Thienothiadiazole Units: Synthesis, Optical, and Electrochemical Properties. *J. Polym. Sci., Part A: Polym. Chem.* **2010**, *48*, 2743–2756.

(56) McCarley, T. D.; Noble, C. O.; DuBois, C. J.; McCarley, R. L. MALDI-MS Evaluation of Poly(3-hexylthiophene) Synthesized by Chemical Oxidation with  $\text{FeCl}_3$ . *Macromolecules* **2001**, *34*, 7999–8004.

(57) Wu, D. H.; Chen, A. D.; Johnson, C. S., Jr. An Improved Diffusion-Ordered Spectroscopy Experiment Incorporating Bipolar-Gradient Pulses. *J. Magn. Reson., Ser. A* **1995**, *115*, 260–264.

(58) Crabtree, A. M.; O'Brien, J. F. Excess Viscosities of Binary Mixtures of Chloroform and Alcohols. *J. Chem. Eng. Data* **1991**, *36*, 140–142.

(59) Evans, R.; Deng, Z.; Rogerson, A. K.; McLachlan, A. S.; Richards, J. J.; Nilsson, M.; Morris, G. A. Quantitative Interpretation of Diffusion-Ordered NMR Spectra: Can We Rationalize Small Molecule Diffusion Coefficients? *Angew. Chem., Int. Ed.* **2013**, *52*, 3199–3202.